

Microstructure evolution accompanying high temperature; uniaxial tensile creep of self-reinforced silicon nitride ceramics

Q. Wei ^{a,b,*}, J. Sankar ^a, A.D. Kelkar ^a, J. Narayan ^b

^a *Department of Mechanical Engineering, NSF Center for Advanced Materials and Smart Structures, North Carolina A and T State University, Greensboro, NC 27411, USA*

^b *Department of Materials Science and Engineering, North Carolina State University, Raleigh, NC 27695-7916, USA*

Received 3 May 1999; received in revised form 5 July 1999

Abstract

Extensive transmission electron microscopy (TEM) has been performed to study the microstructure evolution of a self-reinforced silicon nitride associated with high temperature creep. A large population of strain whorls is observed in samples crept at relatively high temperatures and the strain whorls are not necessarily asymmetrical with respect to the grain boundary normal. Large angle convergent beam electron diffraction (LACBED) at the grain boundaries where strain whorl contrast is visible reveals severely curved Bragg lines, implying large residual strains. This indicates that grain boundary interlocking might be effective to enhance the creep resistance at high temperatures. Dislocation pile-ups, arrays and tangles are present in certain silicon nitride grains. However, a simple analysis rules out dislocations as the major creep mechanism. Most dislocations started from grain boundaries. The role of dislocations is to relieve the stress concentrations at the strain whorls. This adds to the diffusion mechanism of stress relaxation at the strain whorls and facilitates other creep mechanisms such as grain boundary sliding. A large density of multiple-junction cavities is observed in the samples crept at relatively high temperatures. It is proposed that grain boundary sliding and cavity formation, in addition to stress relaxation through nucleation of dislocations at the strain whorls act together to produce a much shorter life to failure at high temperatures. While at lower temperatures, the creep is more diffusion controlled which gives a stress exponent of unity. © 1999 Elsevier Science S.A. All rights reserved.

Keywords: Silicon nitride; Ceramics; Self-reinforced; Creep; Microstructure; Dislocations

1. Introduction

One of the most serious problems associated with ceramics is the poor fracture toughness. For the past two decades, enormous effort has been exercised to get around this problem by means of reinforcement [1], phase transformation toughening [2], microstructure designing [3], etc. Among the family of non-oxide ceramics, silicon nitride has been a very important member because of its unique properties. For example, silicon nitride has very high strength, very low thermal expansion coefficient and chemical stability at high temperatures. In the mid 1980s, silicon nitride ceramics with high fracture toughness had been produced through

composition and microstructure design such that the fracture toughness reached $\sim 10 \text{ MPa}\cdot\text{m}^{1/2}$ [4]. Recently, AlliedSignal has produced a new silicon nitride, GS44, with yttria, alumina and magnesia as sintering aids. This material has moderate to high fracture toughness ($8.2 \text{ MPa}\cdot\text{m}^{1/2}$) and quite high room-temperature strength. Elongated grains with an aspect ratio of above seven usually characterize silicon nitride ceramics with high fracture toughness. The elongated grains work in such a way that crack bridging, pull-out of these grains and crack deflection mechanisms effect the reinforcement and lead to much improved fracture toughness [5]. However, not much is known about the creep behavior of this type of silicon nitride.

Using the stress exponent, apparent activation energy and the grain size exponent to determine the rate controlling process of creep deformation of a material can be superficial. This is understood if we bear in mind

* Corresponding author. Tel.: +1-336-3347348; fax: +1-336-3347417.

E-mail address: qwei@eos.ncsu.edu (Q. Wei)

the fact that many factors can contribute to the changes of the stress exponent and the apparent creep activation energy. In this respect, the creep strain rate may be written as [6]

$$\dot{\epsilon} = A(\sigma, T, S, e) \sigma^n \exp\left[-\frac{\Delta H_C(\sigma, T, S, e)}{RT}\right] \quad (1)$$

where the pre-exponential term A , and the activation enthalpy for creep ΔH_C , are functions of stress, temperature, structure, and environment. The structure term S , may include such parameters as grain size, dislocation density and purity, etc.

Therefore, microstructural studies are crucial for the understanding of the creep mechanisms of a material. However, in situ microstructural analysis is not feasible since for ceramics usually the creep temperature is quite high. So far, all the microstructural observations of the crept samples have been done after the samples are cooled down from the creep temperature. One of the advantages of microstructural studies of crept samples is that it is the ideal way to establish the structure–property relationship.

In this paper, transmission electron microscopy (TEM) is used to study the microstructure evolution associated with the creep processes of GS44 at various temperatures and under various load conditions.



Fig. 1. TEM micrograph of GS44 ruptured after 3.95 h of creep at 1275°C under 80 MPa.

2. Experimental details

A detailed description of the creep experiment is given elsewhere [7]. Rod-like creep specimen design was chosen based upon a simple geometry that allowed minimal volume of material, minimum machining, low cost and ease of alignment. All of the specimens had a ground surface finish of 2–3 μm . Tensile creep tests were performed at temperatures from 1100 to 1275°C, under stress levels from 60 to 140 MPa. It was found that at temperatures greater than 1200°C, creep life was much shorter than at lower temperatures under the same stress level. The creep tests yielded an activation energy of 960 kJ/mol and stress exponent of unity at 1100°C, and 2.0 at higher temperatures. The TEM samples were cut from the gauge section of the sample, as close to the fracture surface as possible. The samples were then mechanically polished to 50–80 μm . A dimple was made with the center area being around 10 μm thick. The samples were placed on a molybdenum ring of 3 mm in diameter and ion milled using a dual gun ion-milling machine to electron transparency. Initially, the ion-milling machine was operated at 5 KV and the angle between the ion beam and the sample surface was about 15°. Before loading the specimen into the electron microscope, the samples were cleaned in the ion-milling machine by using 2.5 KV ion beam and 12° to remove any amorphous phase produced by the ion milling process. TEM studies were conducted on TOP-CON-002B operating at 200 KV. Large angle convergent beam electron diffraction (LACBED) technique was also used to study the strains at the grain boundaries.

3. Results and discussion

In our TEM studies, we have observed strain whorls, dislocations, grain boundary sliding, and cavities in certain samples. However, the frequency of occurrence of these phenomena is a function of creep temperature and stress. In the following, various phenomena will be described and discussed separately as pertaining to the creep mechanism of GS44.

3.1. Strain whorls and strains at grain boundaries

Fig. 1 is a bright field electron micrograph showing the microstructure of GS44 ruptured at 1275°C under 80 MPa after 3.95 h of creep. Apart from voids or cavities that will be discussed later, we can see strain whorls that were first reported by Lange et al. [8]. The strain whorls are localized at certain places and most of them are along the grain boundaries. These observations are in general agreement with those of Lange et al. In their work, they stated that in general the strain

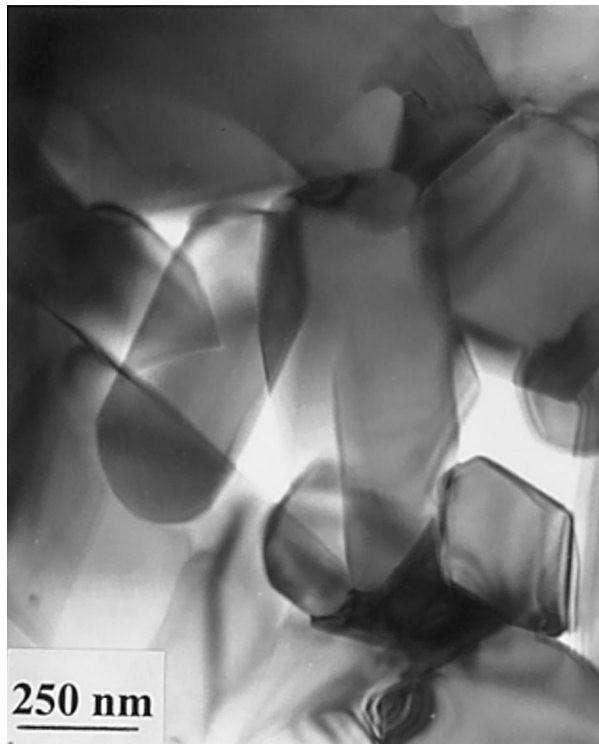


Fig. 2. TEM micrographs showing strain whorls in GS44 ruptured after 3.95 h of creep at 1275°C under 80 MPa. The strain whorls are quite symmetrical with respect to the grain boundary normal.

whorls appeared asymmetrical with respect to the boundary normal. This is not necessarily the case. There are some strain whorls that are quite symmetrical with respect to the grain boundary normal (see Fig. 2, for example). We postulate that whether a symmetrical strain whorl is present or not will depend on the illumination condition in the microscope: the direction of the electron beam with respect to the grain orientation. This is supported by the observation that the strain whorls are essentially extinction contours resulting from a localized out-of-plane buckling of the electron microscope foil [8]. We observed no inclusions or particles in the center of the strain whorls or in close proximity of the strain whorls. Since atomic resolution can not be reached around the strain whorls because of the abrupt changes in the deviation parameter(s) from the exact Bragg condition in the vicinity of the strain whorls, we believe it would not be convincing to simply attribute the strain whorls to the stressed asperities such as ledges of single or multiplanar height at grain boundaries. Another point worthy of attention is that the TEM samples in the present study were prepared from creep samples ruptured at high temperatures (the creep temperatures) and then cooled down to ambient temperature. Whereas in Ref. [8] the samples that showed strain whorls had been cooled under load. Therefore, whether strain whorls can survive the high temperature holding depends not only on whether the

samples are cooled under load or not, it also depends on how easily the concentrated stress condition at the strain whorls can be released. This will depend upon the surroundings of the strain whorl such as the amorphous grain boundary phases, their ability to support the stress and the mechanism for the stress to be released by alternative mechanisms such as diffusional processes. While in silicon nitride ceramics consisting of equiaxial grains, the strain whorl might have originated from the stressed asperities of grain surfaces, in GS44, they might be also due to stress induced contact of two grains, since this material has elongated grains. We can expect that interlocking of silicon nitride grains has a significant contribution to the creep resistance of this material.

One of the distinct features of the creep behavior of in situ reinforced silicon nitride, such as GS44, as compared to other monolithic silicon nitride, is the very high activation energy (960 kJ/mol for this work). This observation is in agreement with other studies on in situ reinforced silicon nitride [9–14]. It falls in a range far beyond the conventional silicon nitride ceramics [15,16] such as sintered, HIPed or reaction bonded silicon nitride ceramics that consist of equiaxed grains. The major difference between the materials is the microstructure. We can therefore presume that large activation energy values are one of the main virtues of self-reinforced silicon nitride associated with the microstructural characteristics. A more detailed model is still needed to explain the high activation energy for in situ reinforced silicon nitride ceramics.

Crampon et al. [12] also observed strain whorls in their samples, and their experiments produced an activation energy very close to ours (960 kJ/mol) while the stress exponent was around unity. They suggested that these are indicative of a solution-diffusion-precipitation accommodated grain-boundary sliding, following the theoretical model of Raj and Chyung [17] where the diffusion through the glass phase is rate controlling. These authors thought that the driving force for diffusion is the chemical potential difference caused by the stress at the strain whorls. Mass transport takes place from the compressed area at the strain whorls to those under tension. The more detailed model for this process is proposed by Wakai [18,19], which can explain the stress exponent of unity.

Strain whorls are also observed in samples crept at lower temperatures such as 1000°C. Fig. 3 is a TEM micrograph showing elongated silicon nitride grains and strain whorls. However, the occurrence of strain whorls at this temperature is less frequent than at 1275°C.

Fig. 4a is an electron micrograph showing a strain whorl along the grain boundary of two silicon nitride grains. Fig. 4b is a portion of a large angle convergent beam electron diffraction (LACBED) disk taken from

the grain boundary of Fig. 4a. Significant bending of the Bragg lines close to the grain boundary where the strain whorl lies indicates that there is very large residual strain around and at the strain whorl. (The traditional methods of convergent electron beam diffraction



Fig. 3. TEM micrograph of GS44 crept at 1000°C under 80 MPa for 500 h without failure. It shows elongated grains and strain whorls of less population as compared to the sample crept at 1275°C.

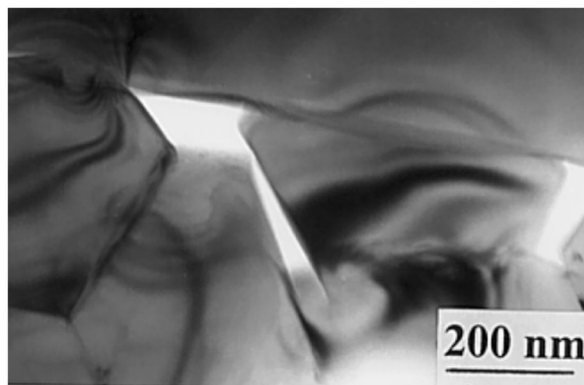


Fig. 4. TEM micrograph showing strain whorls at the grain boundaries (a) and a portion of the large angle convergent electron diffraction disk (b) from (a) showing severely bent Bragg lines close to the grain boundaries where the strain whorls lie.

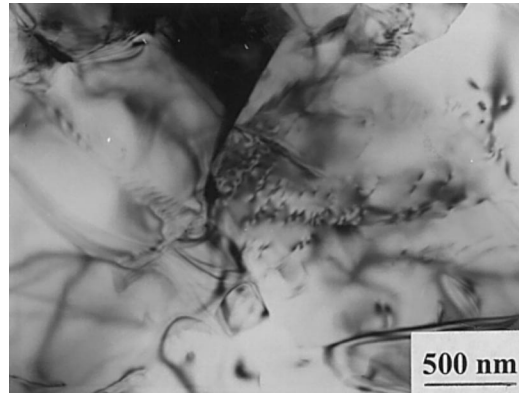


Fig. 5. Dislocation pile-ups in some silicon nitride grains of GS44 crept at 1275°C under 80 MPa for 3.95 h.

(CBED) use a converged probe focused on to a specimen in the object plane resulting in the formation of a CBED pattern in the diffraction plane (the back focal plane of the objective lens). LACBED is a development of CBED which uses a convergent but defocused probe (usually focused below the specimen) forming a shadow image in the diffraction plane, that is the LACBED discs contain low spatial resolution image information superimposed upon high angular resolution diffraction information [20,21].)

Since the occurrence of strain whorls is quite localized, we should expect that the creep deformation of this material accommodated by strain whorls is also localized at a microstructure level.

3.2. Dislocations and their roles in creep deformation

In Ref. [22], the dislocation networks that are observed in virgin GS44 have been described. In the present section, TEM observations of dislocations will be given for the crept samples. Fig. 5 gives the dislocation pile-ups and Fig. 6 shows dislocation arrays in some silicon nitride grains from a sample crept at 1275°C for 3.95 h. Fig. 7 shows dislocation tangles in a silicon nitride grain in the same sample. These images indicate that during creep, some grains underwent plastic deformation through dislocation mechanism. Fig. 8 shows the bright field image of dislocations in a silicon nitride grain imaged under multi-beam condition (a) and their dark field image (b). The inset in Fig. 8a is the selected area diffraction pattern (SADP) taken from the silicon nitride grain that contains the dislocations. The SADP is indexed to come from zone $[1\bar{5}49]$ and is corroborated by calculations using this zone axis. To study the dislocations in Fig. 8 in more detail, systematic diffraction contrast analysis was carried out by tilting the sample in the microscope with reference to the in-zone SADP. Two beam conditions were achieved for dislocation imaging and for the use of the $g \cdot b = 0$ invisibility criterion. The quantitative analysis of dislo-



Fig. 6. Dislocation arrays in a silicon nitride grain of GS44 crept at 1275°C under 80 MPa.

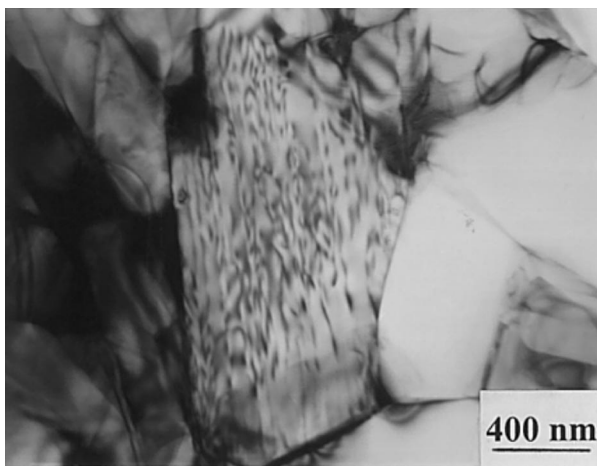


Fig. 7. Dislocation tangles in a silicon nitride grain of GS44 crept at 1275°C under 80 MPa.

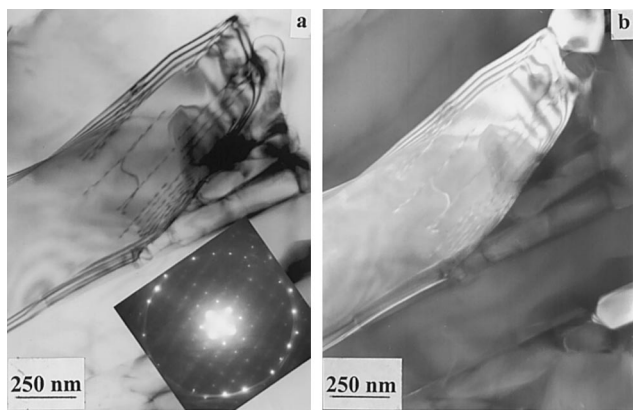


Fig. 8. Multi-beam condition image of dislocations in a beta-silicon nitride grain in GS44 crept at 1275°C with a time to rupture of 3.95 h. Bright field (a) and dark field images of dislocations. Inset in (a) is the diffraction pattern that has a zone axis of $[1\bar{5}49]$.

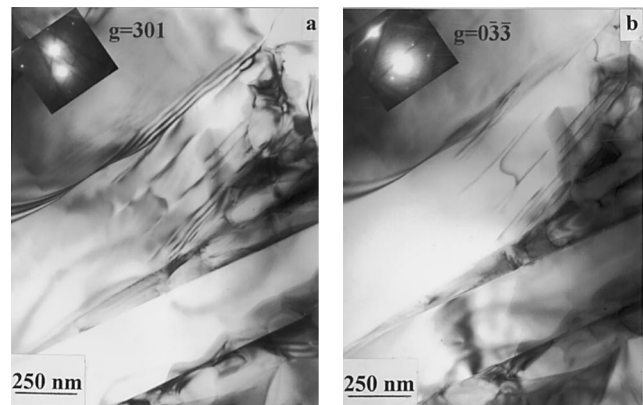


Fig. 9. Two beam diffraction contrast of the dislocations in a grain of beta-silicon nitride. Dislocation are in contrast in both $g = 301$ and $g = 03\bar{3}$.



Fig. 10. Two beam condition bright field image showing dislocations out of contrast with the excited reflection being $g = \bar{3}10$.

cations in a crystal is based on the Darwin–Howie–Whelan equations [23,24], from which the $g \cdot b = 0$ invisibility criterion can be deduced easily. It has been used to identify the Burgers vectors in both beta- and alpha-silicon nitride. Fig. 9 shows the dislocation images acquired under two beam conditions with reflections $g = 301$ and $g = 03\bar{3}$. Fig. 10 is a TEM micrograph from the same area as Figs. 8 and 9. The excited reflection is $g = \bar{3}10$ and the dislocations are out of contrast. It can thus be inferred that the Burgers vector of these dislocations is $c [0001]$. This is in agreement with the results by Butler [25], Evans and Sharp [26], and Milhet et al. [27], that reported most of the dislocations in beta-silicon nitride have the axial Burgers vector and lie in $\{100\}$ planes.

Dislocations have been considered to have little effect on the creep behavior of silicon nitride ceramics, since it has been suggested that at the creep temperatures, dislocation multiplication and movement are not likely to happen. What is more, unlike FCC or BCC metals that have at least five independent slip systems, beta silicon nitride is hexagonal and covalently bonded, and has less than five independent slip systems. However, at elevated temperatures and under fairly large stress, some planes that usually do not slip may come into play. TEM observation has shown not only the axial dislocations having Burgers vector along the [0001] axis [25], non-axial dislocations have also been reported in beta silicon nitride [28]. For example, glide systems such as $1/3 \langle 1\bar{2}10 \rangle \{10\bar{1}1\}$ have been revealed by Milhet et al. [27]. Therefore, it appears that dislocation generation at the interlocking locations might be a plausible mechanism to accommodate the stress and

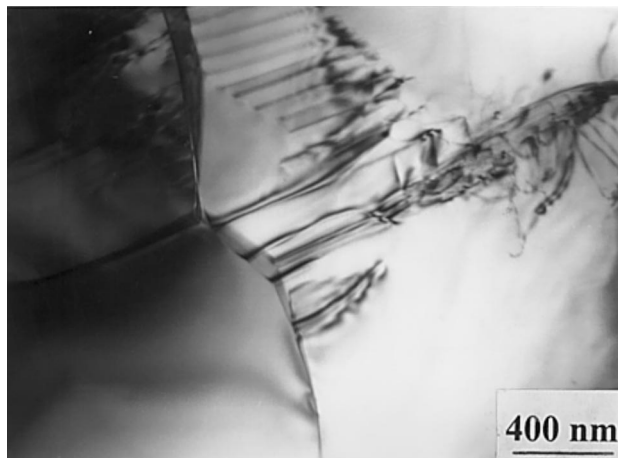


Fig. 11. Dislocations observed in GS44 crept at 1275°C under 80 MPa showing a number of dislocations originated from the grain boundaries.

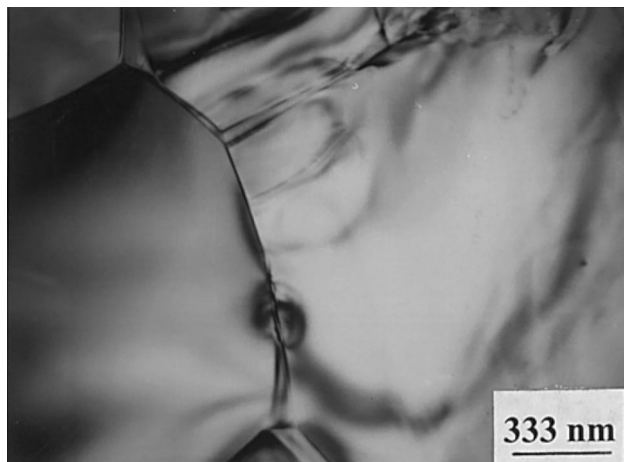


Fig. 12. Strain whorl at the grain boundary and dislocations starting from the grain boundary observed in GS44 crept at 1275°C under 80 MPa.

contribute to the creep strain rate, especially when the creep temperature is high. This seems particularly important in the case of in situ self-reinforced silicon nitride where interlocking effect is expected to be very significant. However, the efficiency of dislocations in this respect needs more detailed consideration. Li and Reidinger [9] also observed dislocations in the crept sample of an in situ reinforced silicon nitride. The authors attributed the creep strain to the step model instead proposed by Waikai [18,19], even though the stress exponent was 3.2.

We propose that at high temperatures and under certain stress conditions, plastic deformation through dislocation movement may be a plausible mechanism. However, because the occurrence of a large density of dislocations is only localized in a few silicon nitride grains, dislocation can not at all account for the major creep strain. The strain due to dislocation motion can be written as

$$\varepsilon = \rho b x \quad (2)$$

where ε is the plastic strain, ρ is the dislocation density, b is the magnitude of the Burgers vector, and x is the average distance a dislocation moved. Considering the localization of dislocations in the crept sample observed in this work, we could safely take an average dislocation density of $10^7/\text{cm}^2$. The magnitude of Burgers vector $b = 3.29 \times 10^{-8}$ cm for axial dislocations, and $x = 0.001$ cm is the average grain size of GS44. The estimated strain is then only of the order of 10^{-4} . This is very minor compared to the total creep strain obtained in this work. It is in accord with the analysis made by Kossowsky [29]. Therefore, dislocation is not the major mechanism for the creep deformation of this material. Here we did not consider the non-axial dislocations since according to Evans and Sharp [26], $\langle 0001 \rangle$ dislocations are the most stable that are also likely to be most mobile with $\{10\bar{1}0\}$ as the primary slip plane.

Nevertheless, the occurrence of dislocations in some silicon nitride grains needs to be addressed in more detail. Fig. 11 shows dislocations in some silicon nitride grains that went through the 3.95 h of creep under 80 MPa. It is interesting to observe that these dislocations are quite close to the grain boundaries. Particularly, we can see certain dislocations start from the grain boundary and the dislocation images extend into the silicon nitride grains. A more careful examination at the dislocation pile-ups shown in Fig. 5 indicates that some pile-up starts from the grain boundary and crossed the whole silicon nitride grain. The strain whorls at both ends of the pile-up are still visible. Fig. 12 shows both a strain whorl and dislocations starting from grain boundary.

In Fig. 13, we can see dislocations starting from places where two silicon nitride grains contact. Around

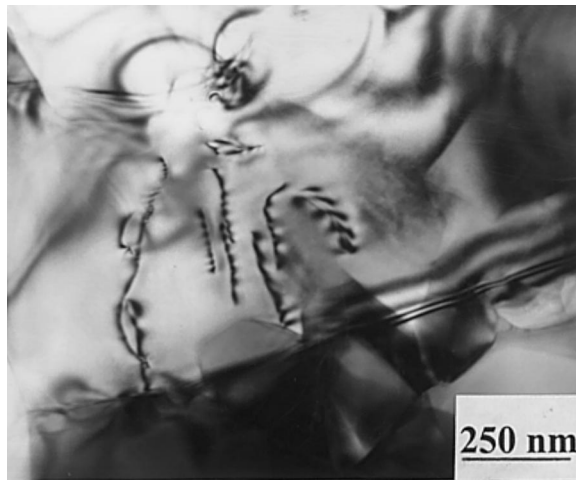


Fig. 13. Dislocations starting from contacting point of two silicon nitride grains. Trace of strain whorl can also be seen at the back end of a dislocation in the lower left corner of the micrograph.

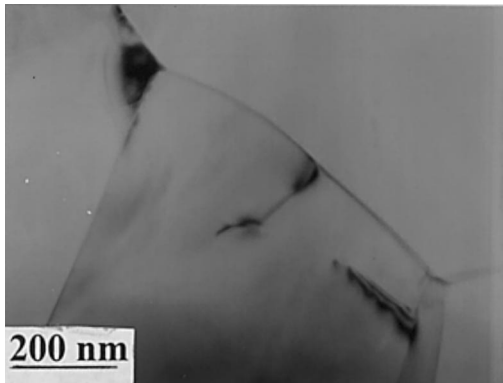


Fig. 14. Two dislocations starting from the grain boundaries and their images extended into the silicon nitride grain.

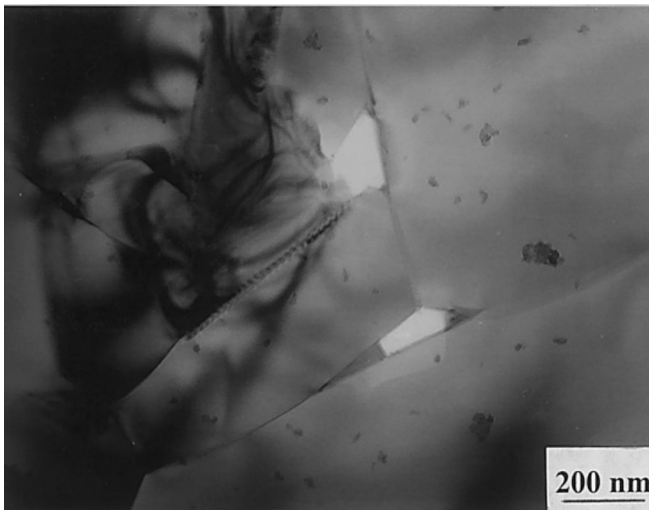


Fig. 15. Cavities in GS44 crept at 1100°C for 500 h under 80 MPa.

the dislocation at the lower left corner of the micrograph the trace of a strain whorl is still visible. In Fig. 14, two dislocations are shown to start from the grain boundaries. Here, we see the nucleation of dislocations at the grain boundary.

The significance of the observations of Fig. 5 through Fig. 13 is that, in addition to the diffusional processes, dislocation nucleation and motion is also an alternative mechanism of stress relaxation at the grain boundaries of silicon nitride in high temperature creep. Even though dislocation mechanism is not responsible for the major creep strain in this silicon nitride ceramics, its effect in relieving the interlocking stress and facilitating other creep mechanism such as grain boundary sliding may accelerate the creep process and contribute to making the time to rupture much shorter for high temperature creep than for lower temperature creep.

3.3. Cavities and grain boundary sliding

Figs. 1 and 2 both show cavities in addition to some other features due to creep. In the samples of the present study, no lenticular (penny-shaped) cavities have been observed. While lenticular cavities have usually been observed along the grain boundaries [13,14,30], which indicates severe grain boundary sliding, in this study, all the cavities occur at the multiple junction pockets. Fig. 15 is a TEM micrograph of GS44 crept at 1100°C for 500 h without rupturing. Cavities at two triple junctions are shown. Also visible in this micrograph is the contrast along the grain boundary of two silicon nitride grains that might be attributed to grain boundary sliding, as can be seen from the strain contrast in the close vicinity of the grain boundary. Evidence for grain boundary sliding is seen in Fig. 16, where grain boundary sliding leaving a gap between two grains is indicated.

Recently, a model has been proposed by Lofaj et al. [31], for the cavitation strain contribution to tensile creep in vitreously bonded ceramics, which has been tested for self-reinforced silicon nitride. It was shown that more than 90% of the total tensile strain is from

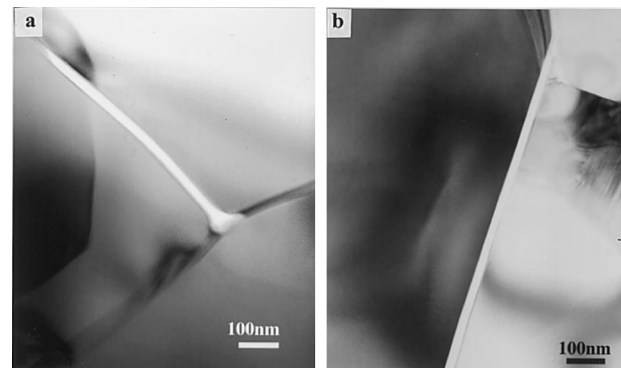


Fig. 16. Direct evidence of grain boundary sliding leaving gaps between two grains of silicon nitride.

cavitation. In his extensive study of the tensile creep in an in situ reinforced silicon nitride ceramics, Gasdaska [10] showed that $\sim 80\text{--}100\%$ of the strain in compression was due to cavitation. However, in the case of tensile creep, the presence and fraction of cavities alone can not account for the total tensile strain of the crept samples. The author proposed that creep strain accumulates by mechanisms in addition to cavitation. He further suggested that some cavity growth must occur by displacement of silicon nitride grains due to sliding. This has been verified in the present work by the direct evidence of grain displacement via grain boundary sliding as shown in Fig. 16. This occurs with reduced viscosity of the grain boundary amorphous phase at high temperatures. Since this kind of grain displacement was rarely observed in the samples crept at lower temperatures such as 1100°C , we might reasonably attribute the reduced creep resistance of this material at higher temperatures to the significant activation of this grain displacement via grain boundary sliding.

In their study on the tensile creep behavior of a HIPed in situ reinforced silicon nitride, Luecke et al. [13,30] observed that the volume fraction of cavities increased linearly with strain and it can be used to account for a substantial fraction of the strain in tension. Though they also observed some lenticular cavities along some grain boundaries, they proposed that the irregularly shaped interstitial cavities made up the bulk of the total volume fraction of cavities. Instead of growth of existing cavities, the addition of new cavities plays a significant role in contributing to the total creep strain. However, at large strains growth of cavities began to contribute significantly to the total volume of cavities.

4. Summary and concluding remarks

Extensive (TEM) studies were conducted on the microstructural evolution of self-reinforced silicon nitride, GS44, associated with high temperature creep processes under different conditions. A large population of strain whorls is observed in samples crept at 1275°C under 80 MPa. The strain whorls are not necessarily asymmetrical with respect to the grain boundary normal. Large angle convergent beam electron diffraction (LACBED) technique showed severely bent Bragg lines close to the grain boundary, implying that grain boundary interlocking may contribute to creep resistance. It is suspected that the large activation energy of self-reinforced silicon nitride ceramics is related to their peculiar microstructure. Dislocation pile-ups, arrays and tangles are present in certain silicon nitride grains crept at 1275°C . However, an analysis of the strain contribution from dislocations shows that dislocations alone can not account for the major creep strain. It is observed that

most dislocations started from grain boundaries. In some cases, the residual contrast of the strain whorls is still visible where dislocations are observed to nucleate. We therefore propose that the major role of dislocations is to relieve the stress concentrations at the strain whorls. This adds to the diffusion mechanism of stress relaxation at the strain whorls and facilitates other creep mechanism such as grain boundary sliding. The dislocation density in the sample crept at 1100°C is much less. A large number of multiple-junction cavities are observed in the samples crept at 1275°C . It is proposed that enhanced grain boundary sliding and cavitation, in addition to stress relaxation through nucleation of dislocation at the strain whorls act together to significantly shorten the life to failure at high temperatures. While at lower temperatures like 1100°C , the creep is more diffusion controlled which gives a stress exponent of unity.

Acknowledgements

This work was sponsored by DOE, Assistant Secretary for Energy Efficiency and Renewable Energy, Office of Transportation Technologies, as part of the Heavy Vehicle Propulsion System Materials Program under contract DE-AC05-96OR22464 with Lockheed Martin Energy Research Corporation. The authors wish to thank Dr Ray Johnson and Dr Ken Liu of ORNL for their continuing support and many helpful suggestions through out this program.

References

- [1] P.F. Becher, *J. Am. Ceram. Soc.* 74 (2) (1991) 255–269.
- [2] P.F. Becher, M.V. Swain, M.K. Ferber, *J. Mater. Sci.* 22 (1) (1987) 76–84.
- [3] K. Hirao, T. Nagaoka, M.E. Brito, S. Kanzaki, *J. Am. Ceram. Soc.* 77 (7) (1994) 1857–1862.
- [4] E. Tani, S. Umebayashi, K. Kishi, K. Kobayashi, M. Nishijima, *Am. Ceram. Soc. Bull.* 65 (9) (1986) 1311–1315.
- [5] P.F. Becher, E.Y. Sun, K.P. Plucknett, K.B. Alexander, C.H. Hsueh, H.T. Lin, S.B. Waters, C.G. Westmoreland, *J. Am. Ceram. Soc.* 81 (11) (1998) 2821–2830.
- [6] R. Kossowsky, D.G. Miller, E.S. Diaz, Tensile and creep strength of hot pressed Si_3N_4 , *J. Mater. Sci.* 10 (1975) 983–997.
- [7] Q. Wei, J. Sankar, J. Narayan, in: 23rd Cocoa Beach Annual Conference of the American Ceramic Society, January 24–29, 1999, Cocoa Beach, FL.
- [8] F.F. Lange, D.R. Clarke, B.I. Davis, Compressive creep of $\text{Si}_3\text{N}_4/\text{MgO}$ alloys, *J. Mater. Sci.* 15 (1980) 611–615.
- [9] C.-W. Li, F. Reidinger, Microstructure and tensile creep mechanisms of an in situ reinforced silicon nitride, *Acta Mater.* 45 (1997) 407–421.
- [10] C.J. Gasdaska, Tensile creep in an in situ reinforced silicon nitride, *J. Am. Ceram. Soc.* 77 (1994) 2408–2418.
- [11] P.J. Whalen, C.J. Gasdaska, R.D. Silvers, The effect of microstructure on the high temperature deformation behavior of sintered silicon nitride, *Ceram. Eng. Sci. Proc.* 11[7,8] (1990) 633–649.

- [12] J. Crampon, R. Duclos, N. Rakotoharisoa, Creep behavior of $\text{Si}_3\text{N}_4/\text{Y}_2\text{O}_3/\text{Al}_2\text{O}_3/\text{AlN}$ alloys, *J. Mater. Sci.* 28 (1993) 909–916.
- [13] W.E. Luecke, S.M. Wiederhorn, B.J. Hockey, R.E. Krause Jr., G.G. Long, Cavitation contributes substantially to tensile creep in silicon nitride, *J. Am. Ceram. Soc.* 78 (1995) 2085–2096.
- [14] S.M. Wiederhorn, B.J. Hockey, D.C. Cranmer, R. Yeckley, Transient creep behavior of hot isostatically pressed silicon nitride, *J. Mater. Sci.* 28 (1993) 445–453.
- [15] W.R. Cannon, T.G. Langdon, Review: creep of ceramics, part 1: mechanical characteristics, *J. Mater. Sci.* 18 (1983) 1–50.
- [16] W.R. Cannon, T.G. Langdon, Review: creep of ceramics, part 2: an examination of flow mechanisms, *J. Mater. Sci.* 23 (1988) 1–20.
- [17] C.K. Chyung, R. Raj, Solution-precipitation creep in glass ceramics, *Acta Metall.* 29 (1981) 159–166.
- [18] F. Wakai, Step model of solution-precipitation creep, *Acta Metall. Mater.* 42 (1994) 1163–1172.
- [19] F. Wakai, N. Kondo, Solution-precipitation creep model for superplastic ceramics with intergranular liquid film, in: R.C. Bradt, C.A. Brookes, J.L. Routbort (Eds.), *Plastic Deformation of Ceramics*, Plenum, New York, 1995, pp. 269–277.
- [20] J.M.K. Wiezorek, A.R. Preston, S.A. Court, H.L. Fraser, C.J. Humphreys, Burgers vector determination of decorated dislocations in $\alpha\text{-TiAl}$ by diffraction contrast and large-angle convergent-beam electron diffraction, *Phil. Mag. A* 69 (1994) 285–299.
- [21] M. Tanaka, M. Terauchi, T. Kaneyama, *Convergent Beam Electron Diffraction-II*, JEOL, Tokyo, 1988.
- [22] Q. Wei, J. Sankar, A.D. Kelkar, J. Narayan, in: *Proceedings of the 38th AIAA/SDM*, 1997, pp. 971–979.
- [23] J.W. Edington, *Practical Electron Microscopy in Materials Science*, van Nostrand Reinhold Company, 1976, pp. 109.
- [24] J. Cowley, *Diffraction Physics*, second, North Holland, Amsterdam, 1981.
- [25] E. Butler, Observation of dislocations in β -silicon nitride, *Phil. Mag.* 21 (1971) 829–834.
- [26] A.G. Evans, J.V. Sharp, Microstructural studies on silicon nitride, *J. Mater. Sci.* 6 (1971) 1292–1302.
- [27] X. Milhet, H. Garem, J.L. Demenet, J. Rabier, T. Rouxel, Dislocations studies in β -silicon nitride, *J. Mater. Sci.* 31 (1997) 3733–3738.
- [28] P.M. Marquis, E. Butler, Non-axial dislocations in reaction-sintered silicon nitride, *J. Mater. Sci. (Lett.)* 12 (1977) 424–426.
- [29] R. Kossowsky, Cyclic fatigue of hot-pressed Si_3N_4 , *J. Am. Ceram. Soc.* 56 (1973) 531–535.
- [30] S.M. Wiederhorn, W.E. Luecke, J.D. French, Importance of cavitation to the creep of structural ceramics, in: R.C. Bradt, C.A. Brookes, J.L. Routbort (Eds.), *Plastic Deformation of Ceramics*, Plenum, New York, 1995, pp. 479–494.
- [31] F. Lofaj, A. Okada, H. Kawamoto, Cavitation strain contribution to tensile creep in vitreous bonded ceramics, *J. Am. Ceram. Soc.* 80 (1997) 1619–1623.